RSC Advances

RSC Advances

www.rsc.org/advances

ROYAL SOCIETY OF CHEMISTRY

www.rsc.org/advances

ARTICLE TYPE

A new nano-sized calcium hydroxide photocatalytic material for the photodegradation of organic dyes

Shujuan Zhang*

Nano-sized calcium hydroxide ($Ca(OH)_2$) photocatalysts were synthesized by a precipitation method. The as-prepared $Ca(OH)_2$ samples were characterized by X-ray diffraction (XRD), X-ray photoelectron spectroscopy (XPS), scanning electron microscopy 10 (SEM) and transmission electron microscopy (TEM), UV–vis absorption spectroscopy and photoluminescence spectroscopy (PL). The as-obtained $Ca(OH)_2$ samples showed excellent photocatalytic degradation activities against methylene blue (MB) aqueous solution under visible light radiation. Dependence of the 15 activity on various experimental conditions was investigated, and the results suggested promising utilization of the $Ca(OH)_2$ photocatalysts. In addition, the photocatalytic degradation of MB was well fitted to pseudo-first-order kinetics. Therefore, MB was photocatalytically degraded over $Ca(OH)_2$ through indirect dye 20 photosensitization.

Introduction

In the past decade, organic pollutants, which lead to environmental contamination that seriously endangers the entire world, can be effectively removed from wastewater by 25 semiconductor photocatalysis materials with high efficiency, nontoxicity, photochemical stability and low cost. Of the reported semiconductors, oxides (TiO_2, ZnO, WO_3),[1-3] sulfides (MoS_2, ZnS, In_2S_3),[4,5] and halides (AgCl, BiOI)[6,7] have been utilized as photocatalysts to oxidize organic pollutants.[8-11] However, their

30 practical applications are limited by the rapid recombination of photogenerated electron–hole pairs, low quantum yields in reactions, and extremely low responses to visible light. Therefore, it is critical to develop novel photocatalysts. In addition to the above-mentioned photocatalysts, metal hydroxide photocatalysts 35 also showed good photocatalytic properties. For example, Li et al. reported both pure and modified $In(OH)_3$ had excellent photocatalytic activities.[12-14] $Ca(OH)_2$ has been widely used as additive for lubricants and dentistry.[15,16] However, $Ca(OH)_2$ nanomaterials have never been reported as photocatalysts so far. 40 Therefore, we prepared $Ca(OH)_2$ nanoparticles by an original method in this study. The structure and composition of samples were characterized systematically. The nano-sized $Ca(OH)_2$ exhibited strong photodegradation activities against MB solution under both UV and visible lights. Meanwhile, under visible light 45 radiation, such photocatalysis was a surface-related photosensitization process. The effects of basic catalyst on the photocatalytic reaction of MB were analyzed in detail, providing valuable references for other metal hydroxide photocatalysts.

Experimental

50 *Synthesis of $Ca(OH)_2$ samples*

Anhydrous calcium chloride ($CaCl_2$, 10 g) was dissolved in 20 mL of deionized water under stirring. A transparent clear solution was obtained (solution 1). NaOH (7.21 g) was also dissolved in

20 mL of deionized water under stirring to acquire solution 2. Solution 1 was dropwisely added to solution 2 under vigorous stirring at room temperature. The solution gradually became turbid and produced numerous white precipitates. The mixture

5 was continuously stirred for 30 min until $Ca(OH)_2$ was completely precipitated. The resultant mixture was filtrated and washed with deionized water and ethanol. The as-obtained $Ca(OH)_2$ precipitates were air-dried at 120°C for 3 h. *2. Characterization of samples*

10 The phase and composition of the samples were analyzed by X-ray diffraction (XRD, Rigaku D/max 2500, λ=1.5406Å, 40 kV, 40 mA). The size and morphologies were observed by a field emission scanning electron microscope (FESEM, Hitachi, S-4800) and a transmission electron microscope (TEM, Hitachi, H-7650).

15 The accelerating voltages of FESEM and TEM were 10 kV and 100 kV, respectively. The UV–vis absorption spectra were recorded on an HP8453 spectrophotometer equipped with an integration sphere using $BaSO_4$ as the reference. Photoluminescence spectra (PL) were measured using a Cary

20 Eclipse photoluminescence analyzer.

Photocatalytic activity measurement

In a typical experiment, the photocatalytic activity of the samples was measured by the photodegradation of MB solution (10 mg/L) in a reactor (100 mL) with 300 mg samples under

25 visible light irradiation. A 300W Xe lamp was used directly for the photocatalytic reaction, while a 400 nm cutoff filter was employed for visible-light photocatalysis to remove UV light. All the mixtures were stirred at room temperature in dark for 30 min to reach adsorption equilibrium before irradiation, and air was

30 continuously bubbled in the solution to provide O_2 that auxiliarily photodegraded MB molecules over $Ca(OH)_2$. Hydroxyl and superoxide radicals are oxidation species in the photocatalytic system, and superoxide radicals are generated in the presence of

O_2. At a defined time interval, the mixture of $Ca(OH)_2$ and dye

35 solution was extracted and centrifuged to remove $Ca(OH)_2$ particles. The remaining MB solution was analyzed by using a UV-vis spectrophotometer at 665 nm. The removal ratio was calculated by $(C_0 − C)/C_0$, where C is the residual concentration after reaction, and C_0 is the original concentration after

40 adsorption equilibrium.

Measurement of the point of zero charge for Ca(OH)₂

The point of zero charge (PZC) of $Ca(OH)_2$ was measured by the salt titrimetric method. $Ca(OH)_2$ (0.5g) and 1, 2.5, 5, 7.5, 10, 12.5, 15, 17.5 mL of 0.1 mol/L NaOH were added to different beakers,

45 respectively. A certain amount of deionized water was added to the beakers to reach a 20 mL total volume. After stirring for 1 h, these solutions were equilibrated for 4 days at room temperature. The pH of the suspension was measured after stirring for 1 h per day. Then 0.5 mL of 2 mol/L NaCl solutions were added to the

50 above mixtures, respectively. The pH was measured after stirring for 3 h (referred to as pH_1). A curve was plotted with the pH abscissa and ΔpH ordinate (ΔpH = pH - pH_1), based on which the PZC of $Ca(OH)_2$ was calculated.

Hydroxyl radicals measurement

55 The formation of OH· radicals under visible-light irradiation was detected by PL. Samples (5 mg) were added to 80 mL of aqueous solution (0.01 mol/L NaOH, 3 mmol/L terephthalic acid), and stirred for 30 min in dark. At a defined time interval (5 min), the concentration of solution was determined by PL under

60 visible-light irradiation (excited at 325 nm).

Results and discussion

Characterization of photocatalysts

The XRD patterns of the as-prepared sample are exhibited in Fig. 1. Main diffraction peaks are in good agreement with the

65 JCPDS card no. 87-0674 of a typical hexagonal-phase $Ca(OH)_2$ crystal (a=b=3.589 Å, c=4.911 Å, space group P3m1[164]),

which only differ in the stronger intensity of (001) diffraction peak than that of (101), indicating that $Ca(OH)_2$ particles probably prefer to grow along the c-axis. Meanwhile, the dominant (001) facets and the facades of the particles are enclosed by (001) facets. Besides, trace $CaCO_3$ impurities that originated from the reaction of $Ca(OH)_2$ and CO_2 in air were found. The strongest (001) peak was used to calculate the crystal sizes of the samples by the Scherrer equation, and the mean size is 38 nm.
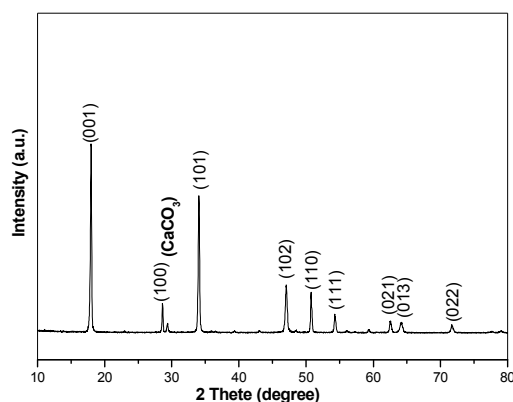
Fig. 1. X-ray diffraction patterns of the as-prepared $Ca(OH)_2$.

As evidenced by the TEM and SEM images of the as-made samples (Fig. 2), the morphology is not monotonous. The irregular nano-sized $Ca(OH)_2$ particles (Fig. 2a) do not agglomerate because they have been ultrasonically dispersed in ethanol. However, single particles consist of these multiple tiny particles. The maximum and the minimum sizes are 75 nm and 20 nm respectively, and the mean size is 35 nm. The as-prepared particles were further measured by SEM in order to investigate the surface morphology. The particles of $Ca(OH)_2$ in Fig. 2b seriously reunite so that they become larger obviously, which may affect the exposure of surface active sites, thereby affecting the photocatalytic activity.
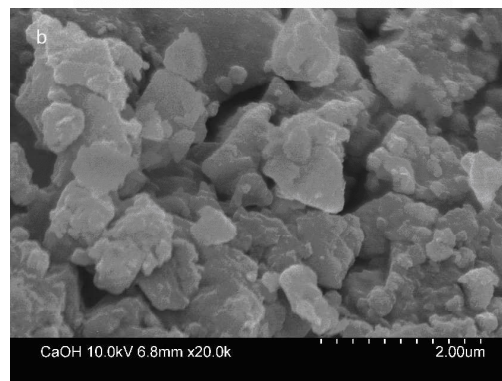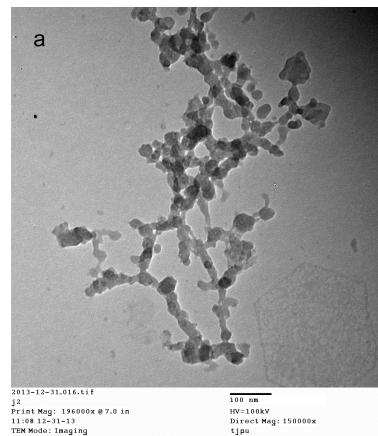
Fig. 2. (a) TEM and (b) SEM images for $Ca(OH)_2$.

Fig. 3A shows the UV-vis absorption spectrum of the as-made $Ca(OH)_2$. There is an apparent, intense absorption edge in the UV light region, and a weak absorption edge can also be discerned in the visible light range. The band gap energy of $Ca(OH)_2$ is estimated as 5.7 eV (Fig. 3B), which indicates that the as-synthesized $Ca(OH)_2$ nanoparticles can hardly be excited by visible light. The valence band of the as-made $Ca(OH)_2$ was measured by XPS, and the peak corresponds to O2p states in $Ca(OH)_2$. It has been previously reported that the binding energy of the onset edge of the O2p peak has an energy gap(E_{vf}) between the valence-band maximum and Fermi level (E_f).[17] The energy gap (E_{vf}) of $Ca(OH)_2$ is approximately 2.5 eV (Fig. 3C), so the energy gap of the conduction-band bottom of $Ca(OH)_2$ is estimated as 3.2 eV by subtracting 2.50 eV from the band gap of $Ca(OH)_2$ (5.7 eV). The Fermi level (E_f), the conduction and the valence bands of $Ca(OH)_2$ are illustrated in Fig. 3D.

band (VB) (D) of the as-synthesized $Ca(OH)_2$.

Fig. 4a and 4b show the PL emission spectra of the as-prepared and commercial $Ca(OH)_2$ samples (about 51 nm for the as-prepared $Ca(OH)_2$; about 0.3 μm for commercial $Ca(OH)_2$), respectively. Only one peak at about 435 nm is observed for the two samples, which is assigned to the transitions band of $Ca(OH)_2$. According to a previous literature,[18] photo-generated electrons in the conduction band that fell into oxygen vacancies through a non-radiation process then recombined with photo-generated holes in the valence band, which thus emitted fluorescence. Since there was only a weak PL emission of $Ca(OH)_2$ (Fig. 4a and 4b), the charge carriers merely recombined slightly. Obviously, the PL peak intensity of the as-prepared $Ca(OH)_2$ is lower than that of commercial $Ca(OH)_2$, inferring that nanosized $Ca(OH)_2$ exhibited enhanced photocatalytic activity by inhibiting the recombination of charge carriers.
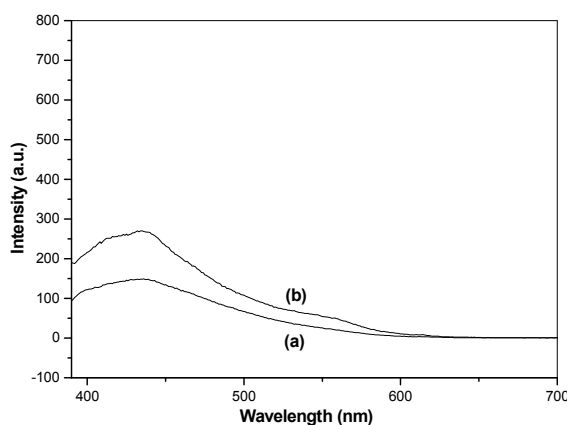
Fig. 4 Fig. 4 PL spectra of $Ca(OH)_2$. (a) The as-synthesized sample; (b) The commercial $Ca(OH)_2$.

Fig. 3. UV-vis absorption spectra (A and B), valence-band XPS spectra (C), and position of conduction band (CB) and valence
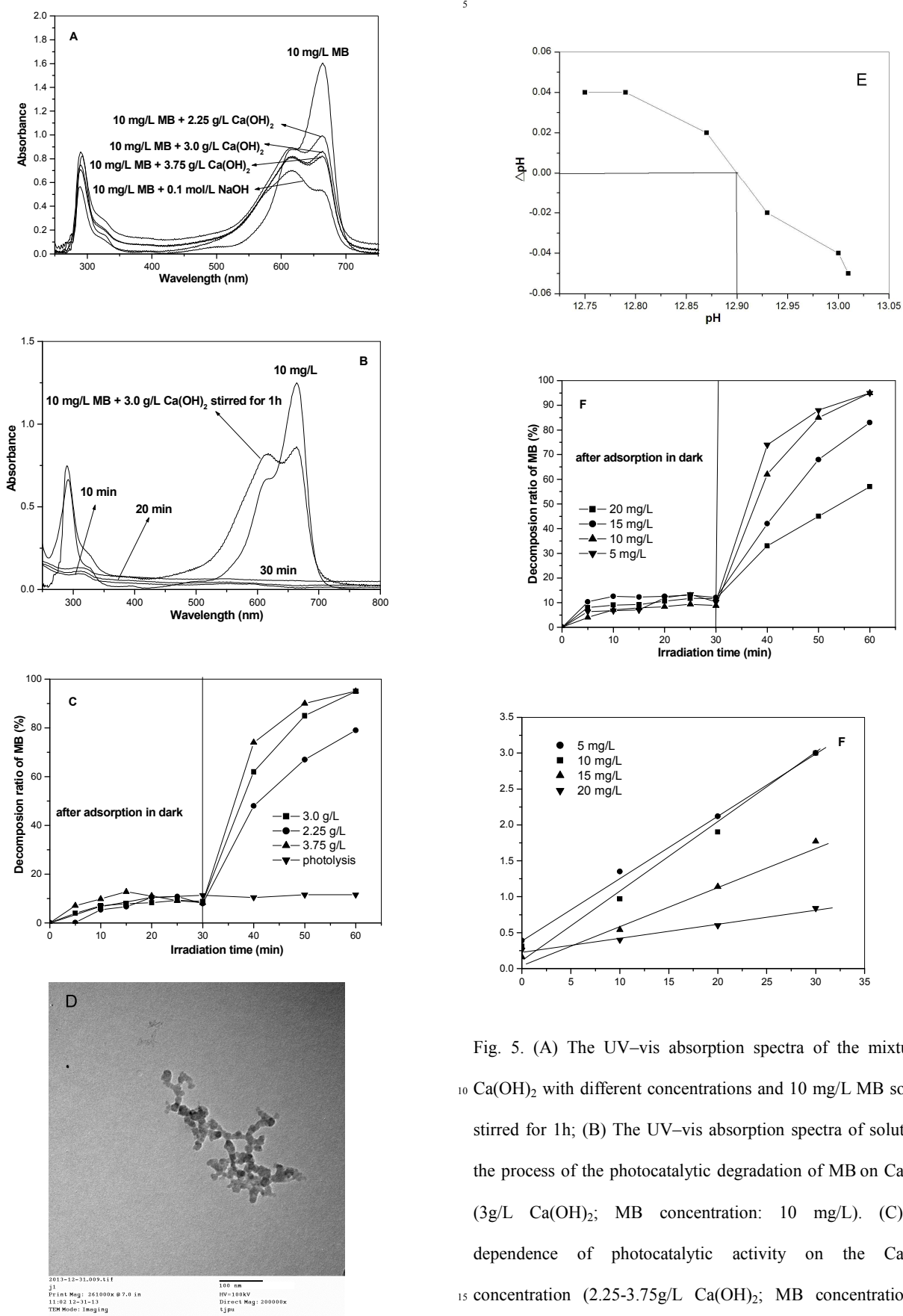
Fig. 5. (A) The UV–vis absorption spectra of the mixture of

10 Ca(OH)$_2$ with different concentrations and 10 mg/L MB solution

stirred for 1h; (B) The UV–vis absorption spectra of solution in

the process of the photocatalytic degradation of MB on Ca(OH)$_2$

(3g/L Ca(OH)$_2$; MB concentration: 10 mg/L). (C) The

dependence of photocatalytic activity on the Ca(OH)$_2$

15 concentration (2.25-3.75g/L Ca(OH)$_2$; MB concentration: 10

mg/L). (D) The TEM image of $Ca(OH)_2$ nanoparticles after irradiation. (E) The point of zero charge (PZC) of $Ca(OH)_2$. (F) The dependence of photocatalytic activity on the original concentration of MB (3g/L $Ca(OH)_2$; MB concentration: 5-20 mg/L). (G) The relationship between $ln(C_0/C_t)$ and irradiation time (3g/L $Ca(OH)_2$; MB concentration: 5-20 mg/L).

Tab. 1 pH of 100 mL of 10 mg/L MB solution

Solution	MB	MB + 0.1 mol/L NaOH	MB + 2.25 g/L $Ca(OH)_2$	MB + 3.0 g/L $Ca(OH)_2$	MB + 3.75 g/L $Ca(OH)_2$
pH	7.0	12.72	12.22	12.41	12.44

Photocatalytic activity of photocatalysts

According to previous literatures,[19,20] we measured the pH values of the mixture of $Ca(OH)_2$ at different concentrations and 10 mg/L MB solution stirred for 1 h (Tab. 1). The pH values of the mixed solution were higher than 12. Fig. 5A shows the UV-visible spectra of the mixed solution. The two absorption peaks at 290 and 665 nm can be assigned to the characteristic structure of MB molecules. The maximum absorption peaks at 665 nm were significantly lower because some MB molecules had been converted into methylene violet (MV) under alkaline conditions.[19,20] However, the absorbance of the degraded solution remained constant (close to zero) with increasing reaction time (Fig. 5B), which may be attributed to further degradation of remnant dye molecules under natural light radiation owing to trace $Ca(OH)_2$ in solution. Hence, MB and MV molecules were degraded over $Ca(OH)_2$ under light radiation. In other words, the decay of MB did not affect the photodegradation rate of MB over $Ca(OH)_2$ obviously. Since MB is a type II photosensitizing dye,[21] a blank experiment was also carried out to investigate the effect of MB on photolysis (Fig. 5C). The photolysis rate ranged from 6.86% to 10.5% without $Ca(OH)_2$ after 10 min of visible light radiation, and the values remained constant thereafter. Therefore, the photolysis of MB

molecules barely affected photodegradation. Total organic carbon (TOC) value in the photodegradation of MB over $Ca(OH)_2$ was also investigated. The concentrations of MB and $Ca(OH)_2$ are 10 mg/L and 3 g/L, respectively. The TOC value of the original MB solution (10mg/L) is approximately 5.181 mg/, and that of MB solution is around 3.951 mg/L after 30 min. Accordingly, MB molecules had been photodegraded in the photocatalytic reaction. In addition, $K_{sp}[Ca(OH)_2]$ of 5.5×10^{-6} may affect the dissolution of particles in aqueous solution. Therefore, the shape and size of particles after irradiation were analyzed by TEM. The maximum and the minimum sizes were 29 nm and 15 nm respectively, and the mean size was 19 nm (Fig. 5D). These sizes were significantly reduced after irradiation in comparison with those of the fresh $Ca(OH)_2$ particles (Fig. 2a) due to low solubility and insufficient stirring.

Various amounts of $Ca(OH)_2$ (2.25 to 3.75 g/L) were added to find out the one that led to the highest photodegradation activity. Fig. 5C shows that the adsorption capacities of the three reactions remain constant after 20 min, suggesting that the adsorption in dark had reached equilibrium. The highest adsorption capacities of the three reactions are 10.8%, 9.4% and 12.8% respectively, which may be associated with the surface charge of $Ca(OH)_2$ colloidal particles as well as the surface group and charge of MB in water. The PZC of $Ca(OH)_2$ was measured by the salt titrimetric method. Fig. 5E shows that the PZC of $Ca(OH)_2$ is 12.9. The pH increases slightly from 12.73 to 12.83 during photocatalysis. However, the pH is lower than the PZC of $Ca(OH)_2$ in water, indicating the surface charge of $Ca(OH)_2$ colloidal particles is positive under our experimental conditions. MB is also positively charged owing to the detaching of Cl^- in water. Thus, the high adsorption of MB over $Ca(OH)_2$ can be attributed to the large number of $-NH_2$ group in MB molecules rather than the surface charge. The high MB adsorption capacity

over $Ca(OH)_2$ facilitated the degradation because the catalytic reaction occurred on the surface. However, since the surface of $Ca(OH)_2$ was not blue after the reaction, the MB molecules adsorbed on the surface had also been degraded despite of the high adsorption capacity. Fig. 5C also reveals that the photodegradation ratio is the highest when 3.75 g/L $Ca(OH)_2$ was added to the solution. However, the photocatalytic activity was not significantly improved after 30 min compared to that of 3 g/L catalyst. Therefore, 3 g/L $Ca(OH)_2$ was selected to perform the photocatalytic reaction.
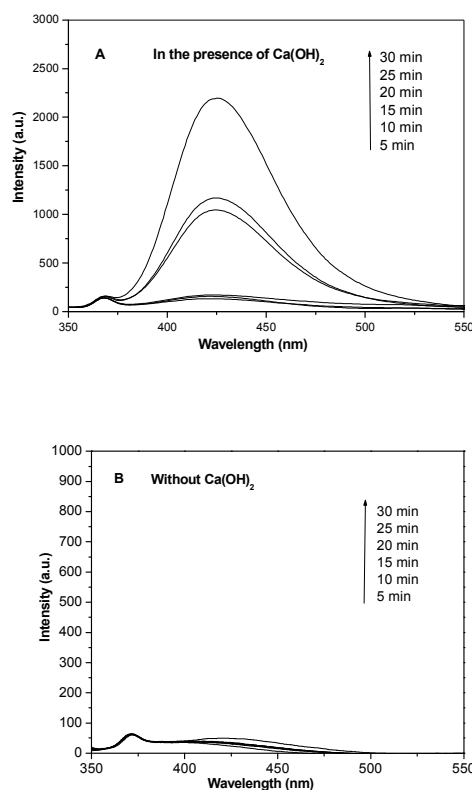
Fig. 6. The PL signal peaks of ·OH radicals at 425 nm.

Moreover, MB solutions at initial concentrations ranging from 5 to 20 mg/L (3 g/L $Ca(OH)_2$) were used. Similarly, the four reactions reached adsorption equilibria after 30 min of stirring in dark (Fig. 5F). As shown in Fig. 5F, the photodegradation ratios are 95, 95, 83 and 57% after 30 min, respectively. The photodegradation activities are highest in the presence of 5 and

10 mg/L $Ca(OH)_2$, and the degradation efficiency decreases with increasing concentration of MB. The $\ln(c_0/c)$ values of MB are linearly correlated with the irradiation time, indicating the photodegradation is a pseudo-first-order reaction (Fig. 5G). The fitting parameters of MB photodegradation kinetics are listed in Tab. 2. The rate constants of photodegradation are calculated as 0.093, 0.077, 0.06 and 0.02 min^{-1}, revealing a rising photocatalytic activity order with decreasing initial MB concentration.

Tab. 2 Relating kinetic parameters on the photodegradation of MB

$Ca(OH)_2$ concentration	k (min^{-1})	R^2
5 mg/L	0.093	0.9962
10 mg/L	0.077	0.9914
15 mg/L	0.06	0.9970
20 mg/L	0.02	0.9683

Hydroxyl radicals (·OH) and photocatalytic mechanism

•OH radicals after visible light irradiation were examined by PL to clarify the active species during the photodegradation of $Ca(OH)_2$. Fig. 6 exhibits the dependence of the PL spectrum of terephthalic acid solution on irradiation time. The PL intensity at 425 nm gradually rose with increasing irradiation time in the presence of $Ca(OH)_2$ (Fig. 6A), indicating that fluorescence was enhanced by the reaction of terephthalic acid with •OH produced by $Ca(OH)_2$ photocatalysis. Fig. 6B shows that water produces •OH under visible light irradiation without $Ca(OH)_2$, and low intensity at 425 nm can be observed, indicating that the increase of •OH in water resulted from $Ca(OH)_2$.

Fig. 3 exhibits that $Ca(OH)_2$ particles cannot be excited by visible light because of a wide gap band (5.7 eV). Therefore, the photocatalysis of $Ca(OH)_2$ resulted from indirect dye photosensitization rather than photoinduced charge carriers. Previous studies have reported that indirect dye photosensitization degradation included photoexcitation of dye molecules, injection of photoexcited electrons into the conduction

band of $Ca(OH)_2$, and capture of the injected electrons by surface-adsorbed O_2 molecules that produces active species ($O_2^{-\bullet}$, OH·, etc.) for the degradation of organic compounds.[22,23] The valence band of $Ca(OH)_2$ does not participate in the photoreaction during photosensitization. Notably, dye molecules directly interact with the semiconductor during the injection of photoexcited electrons into the conduction band of $Ca(OH)_2$. Therefore, the adsorption of a large number of MB molecules on surface of $Ca(OH)_2$ particles (Fig. 5C and 5D) is conducive to photosensitization, which boosts the photocatalytic activity of $Ca(OH)_2$.

Conclusion

In short, $Ca(OH)_2$ nano-photocatalytic materials have been prepared by a traditional method. The average size of the as-obtained $Ca(OH)_2$ particles was about 52 nm. The as-prepared $Ca(OH)_2$ particles absorbed intensely in the visible region. The decreased TOC values of MB solution after a photocatalytic reaction suggested complete photodegradation activities over $Ca(OH)_2$. The MB solution was subjected to slight pH changes during photodegradation, which did not affect the photocatalytic activities obviously. The high adsorption of MB over $Ca(OH)_2$ can be attributed to the $-NH_2$ group in MB molecules instead of their surface charge. The $Ca(OH)_2$ samples were of superior photodegradation activity against MB. Besides, the photocatalytic degradation of MB was well fitted to pseudo-first-order kinetics, and the photocatalytic degradation of MB over $Ca(OH)_2$ was an indirect dye photosensitization process.

[1] Asahi, R.; Morikawa, T.; Ohwaki, T.; Aoki, K.; Taga, Y. Science **2001**, *293*, 269.

[2] Khan, S.U.M.; Al-Shahry, M.; Ingler, W.B. Science **2002**, *297*, 2243.

[3] Justicia, I.; Ordejon, P.; Canto, G. Adv. Mater. **2002**, *14*, 1399.

[4] Zhang, Y.; Li, Y.D. J. Phys. Chem. B **2004**, *108*, 17805.

[5] Zhao, Q.R.; Xie, Y.; Zhang, Z.G.; Bai, X. Crystal Growth & Design, **2007**, *7*, 153-158.

[6] Wang, P.; Huang, B. B.; Qin, X. Y.; Zhang, X. Y.; Dai, Y.; Whangbo, M. H. A Inorg. Chem. **2009**, *48*, 10697.

[7] Wang, P.; Huang, B. B.; Qin, X. Y.; Jin, H.; Dai, Y.; Wang, Z. Y.; Wei, J. Y.; Zhan, J.; Wang, S. Y.; Wang, J. P.; hangbo, M. H. Chem. Eur. J. **2009**, *15*, 1821.

[8] Xi, G.C.; Ye, J.H.; Ma, Q.; Su, N.; Bai, H.; Wang, C. I. J. Am. Chem. Soc. **2012**, *134*, 6508.

[9] Yang, L.Y.; Dong, S.Y.; Sun, J.H.; Feng, J.L.; Wu, Q.H.; Sun, S.P. J. Hazard. Mater. **2010**, *179*, *438*.

[10] Yi, Z.G.; Ye, J.h.; Kikugawa, N.; Kako, T.; Ouyang, S.X.; Williams, H.S.; Yang, H.; Cao, J.Y.; Luo, W.J.; Li, Z.S.; Liu, Y.; Withers, R.L. Nat. Mater. **2010**, *9*, 559.

[11] Bi, Y.P.; Ouyang, S.X.; Umezawa, N.; Cao, J.Y.; Ye, J.H. J. Am. Chem. Soc. **2011**, *133*, 6490.

[12] Hu, S.W.; Zhu, J.; Wu, L.; Wang, X.X.; Liu, P.; Zhang, Y.F.; Li, Z.H. J. Phys. Chem. C **2011**, *115*, 460.

[13] Li, Z.H.; Dong, H.; Zhang, Y.F.; Dong, T.T.; Wang, X.X.; Li, J.Q.; Fu, X.Z. J. Phys. Chem. C **2008**, *112*, 16046.

[14] Li, Z.H.; Dong, T.T.; Zhang, Y.F.; Wu, L.; Li, J.Q.; Wang, X.X.; Fu, X.Z. J. Phys. Chem. C **2007**, *111*, 4727-4733.

[15] Delfort, B.; Born, M.; Chive´, A.; Barre´, L. J. Colloid Interf. Sci. **1997**, *189*, 151.

[16] Shin, H.G.; Kim, H.; Kim, Y.N.; Lee, H.S. Curr. Appl. Phy. **2009**, *9*, S276.

[17] Cao, Y.; He, T.; Chen, Y.; Cao, Y. J. Phys. Chem. C **2010**, *114*, 3627.

[18] Li, D.; Haneda, H.; Hishita, S.; Ohashi, N. Chem. Mater. **2005**, *17*, 2588.

[19]Mills, A.; Hazafy, D.; Parkinson, J.; Tuttle, T.; Hutchings, M. G. Dyes and Pigments **2011**, *88*, 149.

[20]Adamcíková, L.; Pavlíková, K.; Seveík, P. React. Kinet. Catal. Lett. **2000**, *69*, 91.

[21]Wilkinson, F.; Phillip Hellman, W.; Ross, A. B. J. Phys. Chem. Ref. Data **1993**, *22*, 113.

[22] Zhao, J.C.; Chen, C.C.; Ma, W.H. Top. Catal. **2005**, *35*, 269.

[23] Chen, C.C.; Zhao, J.C.; Ma, W.H. Chem. Soc. Rev. **2010**, *39*, 4206.

A new nano-sized $Ca(OH)_2$ photocatalysts with excellent photocatalytic activity.